PROCESSING OF SHUTTLE LASER ALTIMETER RANGE AND RETURN PULSE DATA IN SUPPORT OF SLA-02

Claudia C. Carabajal[1], David J. Harding[2], Scott B. Luthcke[3], Waipang Fong[4], Shelley C. Rowton[5], and J. J. Frawley[6]
[1]NVI, Inc., @ NASA/Goddard Space Flight Center (Code 926), claudia@stokes.gsfc.nasa.gov
[2]NASA/Goddard Space Flight Center (Code 921), harding@denali.gsfc.nasa.gov
[3]Raytheon ITSS, @ NASA/Goddard Space Flight Center (Code 926), sluthcke@geodesy2.gsfc.nasa.gov
[4]Raytheon ITSS, Greenbelt, MD 20770, USA, waipang@magus.stx.com
[5]Raytheon ITSS, Greenbelt, MD 20770, USA, srowton@magus.stx.com
[6] Herring Bay Geophysics, @ NASA/Goddard Space Flight Center, hbgjjf@ltpmail.gsfc.nasa.gov

KEY WORDS: space-borne laser altimetry, remote sensing, laser bounce-point geolocation, laser backscatter modeling.

ABSTRACT

The second flight of the Shuttle Laser Altimeter (SLA) flew on board the space Shuttle Discovery, during August 1997 during the STS-85 Mission. The nearly 3 million laser shots transmitted during the course of the 11 day SLA-02 mission yielded approximately 590,000 geolocated returns from land and more than 1,500,000 from ocean surfaces. These data were analyzed to produce a data set that provides laser altimetry elevations of high vertical accuracy that can be used for scientific purposes. Processing of the data included the geolocation of surface returns, involving precision TDRSS-tracking based Shuttle orbit determination and pointing bias calibration, ellipsoid to geoid reference frame transformations, conversion of engineering parameters to physical units, application of scaling factors to obtain a consistent measure of the backscatter energy, and classification of the returns based on comparisons with reference elevation data (TerrainBase Digital Elevation Model (DEM) and mean sea level). Additionally, the digitized laser returns were analyzed and modeled using constrained non-linear least-squares optimization techniques. The elevation data were compared to both high-resolution DEMs and a reference ocean surface to assess data accuracy. Ancillary data, such as NDVI (Normalized Digital Vegetation Index) and Land Cover classification data, were also included in the distributed data set. Key aspects of the data analysis are discussed. Further documentation concerning SLA-02 data processing procedures, problems evidenced in the data, and its distribution format is provided in the SLA-02 site (http://denali.gsfc.nasa.gov:8001/).

1. INTRODUCTION

The Shuttle Laser Altimeter (SLA) was designed as a pathfinder experiment to evaluate engineering and algorithm techniques to aid the transition of the airborne laser altimeter and lidar technology developed at Goddard Space Flight Center to low Earth orbit operational space-borne systems (Garvin et al., 1996). Two flights of SLA have provided high-resolution, orbital laser altimeter observations of terrestrial surfaces that constitute scientific data sets of value in addressing global Earth System science issues. SLA also serves as a test-bed for upcoming orbital laser altimeters, such as the Multi-Beam Laser Altimeter (MBLA) (Bufton et al., 1999) and the Geoscience Laser Altimeter System (GLAS), that will be launched aboard the Vegetation Canopy Lidar (VCL) mission in 2000 and the Ice, Cloud and land Elevation Satellite (ICESat) in 2001, respectively. The equatorial observations provided by the first flight of SLA (SLA-01) were extended to 57 degrees by SLA-02, characterizing ocean, land, and cloud top elevations in 100 meter diameter footprints spaced every 700 meters utilizing a laser transmitter firing at a rate of 10 pulses per second (Figure 1). The SLA instrument provides the round-trip travel distance of short duration (1064nm wavelength) laser pulses to the first encountered surface, either a cloud top, vegetation canopy top, bare ground, or water, with a 0.75 m precision (Bufton et al., 1995). As for SLA-01, ranging was augmented by digitizing the time-varying return pulse energy from surfaces distributed vertically within the laser footprint, enabling a measurement of within-footprint relief introduced by vegetation cover and topographic slope and roughness. Combining the laser ranging data with shuttle position and pointing knowledge yielded highly accurate surface elevation data. The processing procedures involved in producing the SLA-02 data set are summarized here. The processing procedures and data distribution format are fully specified in the documentation accompanying the data set, available for downloading at http://denali.gsfc.nasa.gov:8001/. The data were acquired and processed as 'observations', which represent a continuous period of instrument operation.

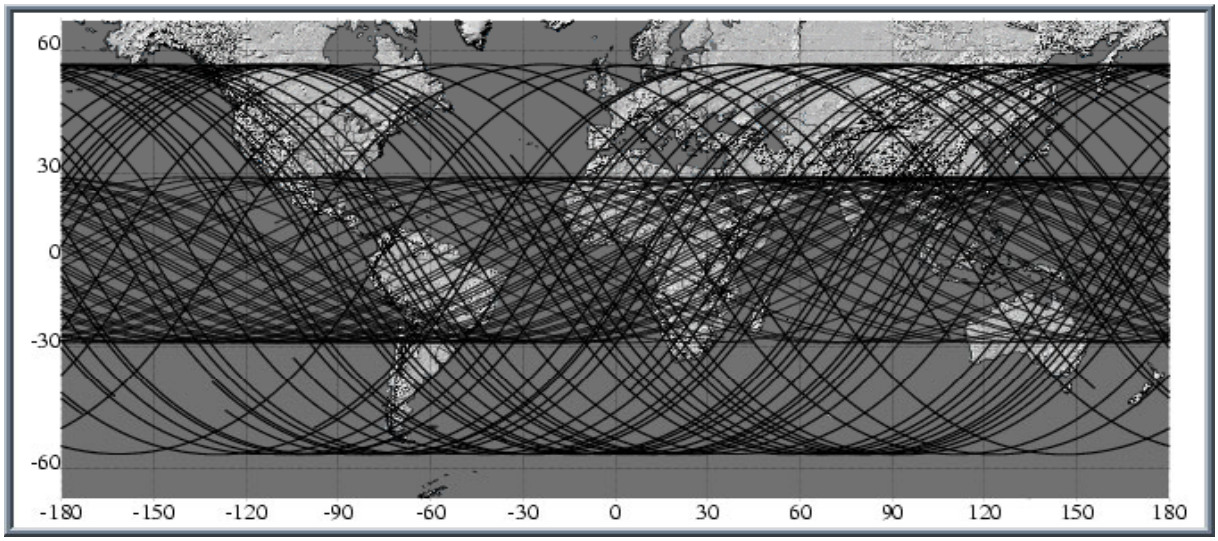

Fig. 1. Map showing Earth surface coverage (all ground tracks obtained) for the two Shuttle Laser Altrimetry (SLA) missions. SLA-02 tracks (57 degrees inclination) are superimposed on equatorial SLA-01 tracks

2. GEOLOCATION PROCESSING

The altimetry geolocation process is extensively treated in Rowlands et al. (1997) and Luthcke et al. (1999); a summary of the process is presented here. The sequential steps used in the geolocation of SLA data are shown in Figure 2.

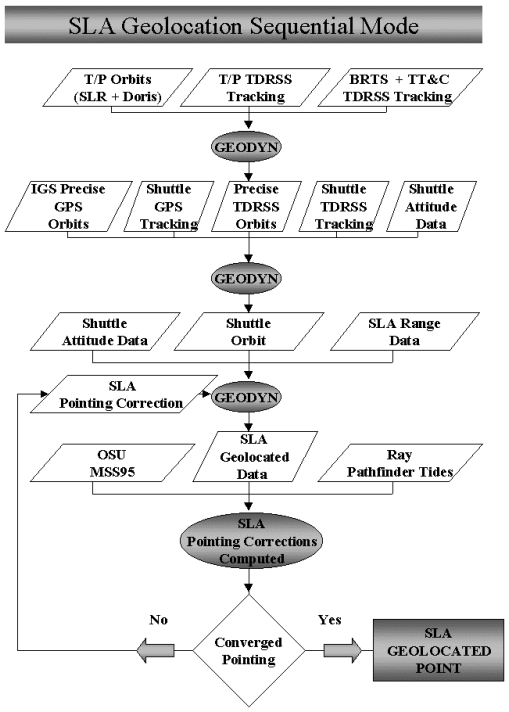

Fig. 2. Diagram showing the sequential steps involved in the geolocation processing of the Shuttle Laser Altimeter data

2.1. Time-tag Data

Before proceeding with the geolocation, time tag data were analyzed to ensure consistent assignment of time to the range data. SLA time is calculated by synchronizing the SLA internal clock with the Shuttle's clock. SLA time provides an incremental time measurement, and the Shuttle's clock provides an absolute time by giving time with respect to the Mission's Reference start time. The Shuttle time is received by SLA as a serial time reference message from the master timing unit, a 4.608-MHz stable crystal-controlled timing source for the orbiter, which provides synchronization for instrumentation payloads and other systems (http://www.ksc.nasa.gov/shuttle/technology/sts-newsref/sts-inst.html). Shuttle time is read and recorded once per minute by the SLA flight software. The SLA internal time is kept by means of an inexpensive oscillator (standard for the flight computer), with a 1.193 MHz frequency. This oscillator acts as a high resolution 16 bit counter which counts down from 65536 to 0, and sends an interrupt to the computer every time it rolls over. In the flight code, for each laser fire the value of the counter and the incremented interrupts are stored. SLA system time is then computed using the following equation:

$$Sys.\ time=[(ticks * 65536.0d0) + (65535.0d0 - hirez)]* *838.09580d-9 \quad (1)$$

For every 1-minute pulse from the Shuttle, the value for hirez, ticks and the Shuttle's 1 pulse-per-minute time are read and stored. This information is combined to produce the laser shot's time-tag. The offset between the Shuttle and SLA time is calculated, and the oscillator's drift is accounted for by fitting the best quadratic function that models the residual of the two time series. The altimeter range time-tags were corrected using this best-fit function. On occasion, the flight software misinterpreted the Shuttle time while unpacking the bytes that contained the minute tag information. This resulted in jumps in

the time line that when easily identified were accounted for and fixed. Duplicate time tags that resulted from a buffering problem during data recording were also identified, and eliminated before geolocation. For several observations (5, 6, 14 and 14a) time-tag inconsistencies have not been resolved, and the data have therefore not been geolocated.

2.2. Shuttle Orbit Determination

In support of SLA-02, meter level Root-Mean Square (RMS) Shuttle radial orbit accuracy has been achieved from Tracking and Data Relay Satellite System (TDRSS) Doppler observations. Traditionally, the Tracking and Data Relay Satellite (TDRS) orbits themselves have been the dominant source of error in Shuttle orbit determination during quiescent attitude periods. The technique utilizing TOPEX/Poseidon's (T/P) precise orbit knowledge, plus the TDRSS-T/P Doppler tracking in conjunction with Biliteration Ranging Transponder System (BRTS) and Telemetry, Tracking and Command (TT&C) range data were used to precisely position the TDRS (Luthcke et al., 1997). Furthermore, a special T/P-TDRSS tracking scenario was devised and implemented in support of the STS-85 mission. This tracking scenario, optimizing the sampling of the TDRS orbits with the best possible tracking data, was not employed for STS-72. The significant improvement in TDRS-4 orbit precision gained from this tracking scenario can be seen in Table 1, when compared to the TDRS orbit precisions obtained in support of STS-72. The TDRS-1 orbit precision is significantly worse than the other TDRS due to that fact that T/P was not tracked by this TDRS. However, nearly all of the STS-85 tracking data was acquired with TDRS-4 and -5.

Mission Supporting	TDRS-1 (m)	TDRS-4 (m)	TDRS-5 (m)
STS-72		4.08	0.82
STS-85	3.57	0.80	0.92

Table 1. TDRS RMS Orbit Overlap Differences; Total Position

Table 2 presents a comparison of model fits to Shuttle-TDRS 2-way range rate data expressed as residual RMS averaged over all orbit arcs during SLA operation. The data shows an improved fit for the STS-85 case. This was mainly due to more relaxed constraints employed for STS-85 and significantly shorter arcs on average. However, it should be noted that the improved fitting of the tracking data does not necessarily indicate improved orbit accuracy.

Mission Supporting	Shuttle-TDRS 2-way range-rate Residual RMS (mm/s)
STS-72	2.37
STS-85	1.41

Table 2. Residual RMS (average over all arcs).

In support of SLA-01, an extensive STS-72 orbit precision and accuracy study was performed (Rowlands et al., 1997). This study showed the shuttle orbits to be accurate to within 1.5 m radial RMS and 8 m total position RMS. From the STS-72 study results, the TDRS orbits precision and shuttle tracking data presented above, and some limited orbit accuracy analysis, the STS-85 orbits are considered to be accurate within 10 m total position RMS and a few meters radial RMS. Ocean comparisons for the first 4 observation periods showed ~2 meter radial orbit accuracy for the well-fit middle of the arcs. The STS-85 orbit accuracies are considered not to be as good as those that were obtained for STS-72 due to shorter arc lengths and significantly more attitude and orbit maneuvers.

2.3. Altimetry Geolocation

Once precise Shuttle orbits are obtained, SLA range data (corrected for a constant range bias and tropospheric effects) are combined with Shuttle attitude data to solve for the laser bounce point location using GEODYN (Rowlands et al., 1993). GEODYN is a state-of-the-art precision orbit determination and geodetic parameter estimation software suite developed at Goddard Space Flight Center. This software suite has been extensively modified to include a rigorous laser altimeter range measurement model and new dynamic cross-over analysis algorithms. The laser bounce point is geolocated using using T/P consistent reference frames, precise shuttle orbits described above, a SLA optical center to Shuttle center-of-gravity offset correction, a -5.6 meters altimeter range bias, and the Marini Murray tropospheric refraction correction. The range used in the geolocation process is the range to the first backscatter signal above the detection threshold. The resulting elevations thus correspond to the highest detected surface within the 100 meters diameter laser footprint. For cloud-free paths to land targets this could be the upper-most canopy where vegetation is present, the tops of buildings or structures, or the highest ground where vegetation, buildings and structures are absent.

2.4. Extracting Pointing Biases

With the excellent shuttle orbit accuracies achieved from the above described precision orbit determination (POD) analysis, the remaining significant factor driving vertical and horizontal geolocation accuracy is the laser pointing knowledge, significantly affected by laser and spacecraft systematic body misalignments. These can be due to mounting offsets, Inertial Measurement Unit (IMU) misalignment, and Shuttle body flexure. An attempt was therefore made to extract pointing biases from the data. The shuttle orientation is maintained during SLA observations by a 'dead band' attitude control system, resulting in SLA pointing controlled to be within either 1 degree or 0.1 degree of nadir. Errors in the a priori Shuttle body attitude, established by an IMU periodically calibrated in-flight by star-camera observations, contribute to the resulting SLA elevation errors, which are significantly larger during 1 degree dead-band modes than during 0.1 degree modes. However, it is considerably easier to both observe and separate the roll and pitch errors during 1 degree dead-band than during 0.1 degree dead-band, even though the increase in attitude hold thrusting required impacts the orbit determination process by

increasing unmodeled dynamical effects. Roll and pitch biases are modeled and corrected before obtaining the final geolocation information. Roll and pitch biases can each be established because Shuttle attitude changes in roll and pitch are significantly out of phase (Luthcke et al., 1999).

A first order approach in recovering pointing and range biases is done using a direct altimetry range residual analysis, combining spacecraft attitude information with ocean range residuals (Luthcke et al. 1999). The direct altimetry ocean data are compared with OSU (Ohio State University) 1995 Mean Sea Surface Model (Yi, 1995), plus the effects of tides from the Ray Ocean Altimeter Pathfinder Tide Model (an extension of the Schrama-Ray Tide Model, 1994), giving a height error for each laser pulse yielding an ocean surface return. Surface elevations of the open ocean are known, through measurements and modeling, to the 12 cm (1 sigma) level, providing a global reference surface to compare to the altimeter range measurements throughout the mission. SLA pointing corrections to the a priori roll and pitch were computed for each of the SLA-02 observation periods, iterating to solve for constant biases that reduce the ocean residuals until convergence was reached. This approach does not include the smaller contributions to ocean surface height variation from barotropic pressure (<10 cm), earth tides (<20 cm) and the time dependent part of dynamic sea surface topography (<50 cm). SLA-ocean surface height differences on the order of 30 meters were typically observed before pointing bias estimation, with larger residuals present in some of the arcs where the Shuttle attitude exhibited a significant number of maneuvers. After establishing the attitude corrections, the bounce point geolocation was recomputed as described above. Average values for the constant attitude biases obtained from the first four observation periods (periods without significant maneuvers) were applied to the data from observations when attitude biases were difficult to extract from the residuals. Data from observation period 17 were geolocated applying no bias corrections for roll and pitch. Figure 3 shows a histogram of the final SLA-02 ocean surface residuals for all observation periods analyzed. The mean and standard deviation of ocean surface residuals is larger for SLA-02 than –01 (Garvin et al., 1998), possibly due to shorter arcs and greater changes in the attitude profiles, which could result in unmodeled time-varying pointing biases during the individual observation periods. In addition, the more frequent attitude and orbit maneuvers during SLA-02 observations may have contributed to increased Shuttle body flexure and non-constant IMU misalignment effects that have not yet been compensated, and made more difficult to de-couple orbit and pointing errors. A much smaller contribution could be attributed to sea surface wave structure, barotropic pressure and solid Earth tides. We are currently in the process of working towards better modeling and recovering these pointing biases and improving the orbits to enhance the geolocation of selected SLA-02 arcs. Leveling Correction and Computing Orthometric Elevations.

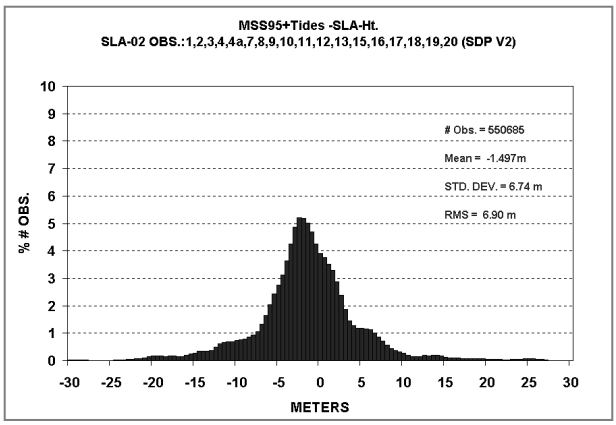

Fig. 3. Histogram of SLA-02 elevation differences with respect to T/P=based Mean Sea Surface ocean topography corrected for ocean tides

A leveling correction is applied to the resulting elevation data for each laser bounce point to correct the effects of long wavelength orbit errors. The ocean range residuals time series is smoothed by a sliding boxcar filter with a window length of 120 seconds. The minimum number of ocean surface laser returns allowed within the window was 50, and a 3 sigma editing of outlier residuals was performed. The resulting ocean leveling correction is extrapolated across land areas using a linear fit to ocean results prior to and after the land. The leveling correction, provided in the sla02.bp.surface_3 parameter, is a measure of the elevation error that is primarily due to long-wavelength orbit errors. The geolocation process yields elevations referenced to the T/P ellipsoid. Orthometric elevations were computed by subtracting the geoid height at each laser bounce-point defined by the Earth Geoid Model 96 (EGM96) (Lemoine et al., 1998). This level of processing constitutes the SLA-02 Standard Data Product Version 2 (SDP v2).

3. ADDITIONAL PROCESSING

3.1. Return Type Classification

Each laser shot was classified according to a scheme that distinguishes returns from ocean or land surfaces based on masks derived from the TerrainBase 5 minute (10 km) resolution global terrain model (Figure 4). Ocean and land shots were each further classified as valid returns, from the Earth surface or clouds, or as non-valid returns, due either to a range return from background noise or a no-range return (no backscatter signal detected above the range acquisition threshold). Ocean surface returns were defined as those whose orthometric elevations did not depart from sea level (elevation = 0) by more than 20 meters. Land surface returns had orthometric elevations within 500 meters of TerrainBase. This larger land elevation threshold was chosen to account for inaccuracies in TerrainBase and geolocation errors causing large elevation discrepancies in high-relief errors. This method probably overestimates the percentage of land surface returns, classifying returns from some low altitude clouds as being from

the surface. Returns classified as clouds included those more than 500 m and 20 m above the TerrainBase and ocean reference surfaces, respectively, and below 10,000 m (considered to be the limit for cloud formation). Returns classified as noise included those 500 m and 20 m below the TerrainBase and ocean reference surfaces, respectively, or above 10,000 m. Figure 4 shows a histogram of the various classification categories for the approximately 2.1 million laser shots that have been geolocated.

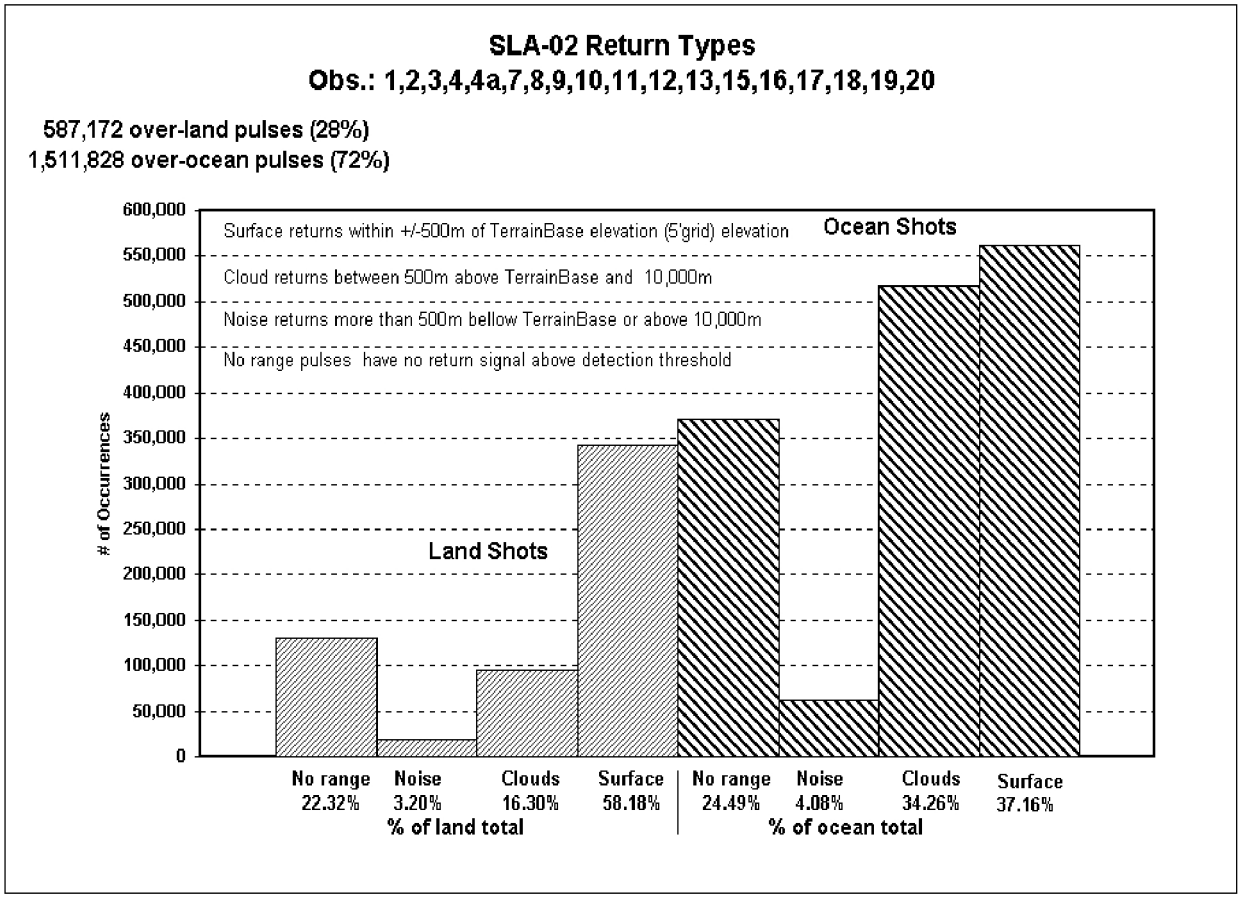

Fig. 4 Number of occurences of SLA-02 return types for all observations processed

The proportion of non-valid returns (noise and no range) was comparable for land and ocean surfaces. The proportion of cloud returns is significantly lower for the land as compared to the ocean, indicative of anomalous, sparse cloud cover over the land areas sampled during the mission. Environmental parameters are also provided in the SLA-02 data set, including ISLSCP land cover class and Normalized Difference Vegetation Index (NDVI), to provide a context for the derived bounce-point geolocation.

3.2. Orientation of the Laser Vector

To allow assessment of off-nadir pointing effects on pulse spreading of the backscatter return, the orientation of the laser vector with respect to the Earth's surface is reported. Once the altimetry data were geolocated, the bounce point topocentric coordinates and shuttle position were used to compute the orientation for each laser vector. The orientation is characterized by the vector's azimuth (horizontal angle of its projection with respect to North) and angle off-nadir (zero in the nadir pointing position), provided in the sla02.pap.azimuth and sla02.pap.aoffnadir parameters of the sla02 structure. Caution should be used when interpreting the values provided for the no-range data, since the geolocation information associated with these is not valid.

4. PROCESSING OF RETURN BACKSCATTER ENERGY

Methods used for the analysis of waveforms acquired during the second flight of the Shuttle Laser Altimeter (SLA) are summarized here. They represent modifications made to codes developed for SLA-01. SLA waveform processing is implemented in the Interactive Data Language (IDL) environment. The methods are dynamic and continue to be modified as experience is gained. Therefore, the following procedures reflect the current SLA 'state-of-the-art' processing. Further discussion of the procedures is described in the documentation distributed with the data set, and we refer the reader to it for more details on the subject.

4.1. Parameterizing the Return Signal

Waveform processing algorithms parameterize the return signal resulting from the interaction of the transmitted laser pulse with the intercepted surface, and identify the response from the multiple targets encountered within the footprint. The SLA detector output voltage is continuously sampled by a high speed, 8-bit digitizer. Upon detection of a backscatter return by the ranging electronics, the digitizer time series is sampled and stored, yielding a waveform record of received laser backscatter energy. The digitizer memory is sampled so as to record detector output voltage beginning slightly before the ranging electronic's detection of the backscatter return and extending in time to include the maximum range of within-footprint heights expected for land surfaces. Thus a time series of the complete backscatter return for land surfaces is recorded. Returns are modeled as a single Gaussian function, or as the combination of several Gaussian peaks when measurement of multiple ranges from a single return is required. In this manner, the vertical extent and approximate height distribution of intercepted surfaces can be derived from the return signal. Most of the waveforms are single peaked and can be fit by a single Gaussian function, characterized by its maximum amplitude, location of this maximum amplitude in time with respect to the ranging electronics detection time, and its half width. When complex surfaces are intercepted within the footprint (as with the presence of complex surface topography, clouds, vegetation, buildings), multiple returns are present in the waveforms and multi-Gaussian functions are used to model these more complex waveforms.

In brief, the waveform **processing steps** consist of:

I) Identifying and processing only shots that are classified as valid surface returns form land and ocean based on a comparison of the laser bounce point elevation (orthometric height) to a reference surface (5 minute resolution Terrain Base Digital Elevation Model for land returns, and mean sea level for ocean returns).

II) Determining the noise baseline and calculating noise mean and standard deviation, establishing a waveform threshold level for signal above noise.

III) Identifying start and end of signal above waveform threshold.

IV) Identifying saturated returns.

V) Subtracting mean noise level from the signal.

VI) Characterizing the basic properties of the signal.

VII) Scaling waveform engineering units to physical units (detector output voltage vs. time) based on scaling factors and calibration constants.

VIII) Identifying returns to be excluded from processing based on anomalous characteristics.

IX) Smoothing the signal.

X) Establishing initial estimates for peak positions, amplitudes and half-widths based on the first and second derivatives of the signal, with exception handling for saturated returns.

XI) Applying constrained function fitting to obtain first estimates of peak amplitudes, with exception handling for saturated returns. Editing peaks based on their amplitude and proximity (zero amplitude peaks are eliminated), with exception handling for saturated shots.

XII) Re-evaluating peak's significance if necessary, and solving for peak amplitude, location, and half-width.

XIII) Deriving distances from the start of the waveform signal to: 1) centroid of all peaks, 2) centroid of the last peak.

For our purpose, a Gaussian peak is defined as follows:

$$F(x) = A(0) * e^{-(z^2/2)}, \quad (2)$$

where $$z = \frac{(x - A(1))}{A(2)}. \quad (3)$$

F is the analytical function representing the model, and the parameters to be solved are:

A(0)= Gaussian peak maximum amplitude
A(1)= location in the time axis
A(2)= 1-sigma deviation from its mean

X_i is the independent variable, Y_i is the observations (independent variables), and ERR_i are the 1-sigma uncertainties in the observations. The residuals are calculated in the following manner:

$$Residuals = (Y_i - F(X_i)) / ERR_I \quad (4)$$

If ERR are the 1-sigma uncertainties in Y, then the total chi-squared value will be:

$$\chi^2 \equiv \sum \left[\frac{Yi - F(xi)}{ERR_i} \right]^2 \quad (5)$$

SLA uses the IDL routine MPFIT to fit Gaussian distributions to the waveform. This is a recently-added, user-supplied IDL routine authored by Craig B. Markwardt, NASA/GSFC Code 622, which uses the The Levenberg-Marquardt technique as a particular strategy to iteratively search for the best fit in the

parameter space (Bevington and Robinson, 1992). A Gaussian distribution is used because SLA does not digitize the shape of the transmitted pulse. Lacking information on the shape of the transmitted pulse on a per shot basis, a Gaussian distribution is used as a reasonable approximation. A non-Gaussian, user-supplied fitting function can be input to MPFIT. Updated versions can be found on http://astrog.physics.wisc.edu/-~craigm/idl.html. MPFIT uses the Levenberg-Marquardt technique to solve the least-squares problem. Within certain constraints, these routine will find the set of parameters which best fits the data in the least-squares sense; that is, the sum of the weighted squared differences between the model and data is minimized by minimizing the Chi-square value, calculating derivatives numerically via a finite difference approximation. A set of starting parameters are specified, and the user can apply constraints to individual parameters by setting boundaries on the lower and/or upper side. Otherwise, it is assumed that all parameters are free and unconstrained. The step size to be used in calculating the numerical derivatives of the model with respect to the parameters can be defined by the user or it is computed automatically, and the covariance matrix can also be computed.

The following constraints are applied during the fitting search: 1) lower bounding constraint that all return position, amplitude and width parameters be non-negative; 2) upper and lower bounding constraints on each peak position such that its final position can not be outside the estimated position bounded by its half-width (stopping peaks from migrating away into larger adjacent peaks); 3) if detector saturation occurs, only that part of the signal up to the saturation point is fit, the estimated peak position is seeded earlier in time to compensate for the falsely broadened return, and the area under the saturated peak is preserved in the Gaussian fit; 4) if the digitizer 8-bit dynamic range is exceeded causing clipping of the signal, then the signal before and after clipping is fit making up for the clipped part of the signal with reasonable accuracy; 5) shots with more than 10 peaks were excluded as they were difficult to fit, usually lacking convergence after 40 iterations (these are probably low-lying cloud returns mis-classified as ocean or land surface returns).

4.2. Deriving Elevations from the Waveform

The SLA ranging electronics provide the range from the start of the transmit pulse to the start of the backscatter return. It is this range that is used in the geolocation processing and, thus, the location of the geolocated bounce point (latitude, longitude, and elevation) refers to the highest detected feature within the 100 m diameter laser footprint. The distances from the start of the waveform signal to the centroid of all the peaks, the centroid of the last peak, and the end of signal, all provided in the SLA-02 data structure, can be used to correct the bounce point elevation depending on the character of the return signal (e.g., single or multi-peaked), the assumed nature of the surface type, and the intent of the end user.

For a measure of the mean elevation of illuminated surfaces within the laser footprint (assuming uniform reflectance of all the surfaces at the 1064 nm laser wavelength) the appropriate range would be from the centroid of the transmit pulse to the centroid of the backscatter return. An approximation of this mean elevation is obtained by:

[geolocated bounce point elevation] + [transmit pulse centroid] – [centroid distance for all return peaks] (6)

The transmit pulse centroid corresponds to the distance from the start to the centroid of the transmit pulse. SLA does not provide a digitized record of the transmit pulse. However, the transmit pulse impulse response can be obtained from returns from flat, smooth surfaces such as water, defining the narrowest possible returns which have not been broadened in time by surface relief. The impulse response pulse width is a function of peak amplitude. Examination of a plot of waveform centroid versus peak amplitude for single-peak returns defines an envelope of data points, with the minimum boundary defining the impulse response centroid which varies from 2 meters for low amplitude returns to 4 meters for high amplitude returns.

For multiple-peaked waveforms where it is assumed that the last waveform peak is due to laser energy backscattered from the ground and that preceding peaks are energy returned from higher surfaces such as vegetation or buildings, the mean elevation of the ground surface can be approximated by:

[geolocated bounce point elevation] + [transmit pulse centroid] – [centroid distance to last peak] (7)

Inference that the last peak corresponds to the ground surface within a 100 m diameter footprint requires that the height distribution is simple, as for example due to an open vegetation canopy or building above a flat ground surface. Ground slope across the footprint can cause convolution of the ground return with returns from overlying surfaces.
For a measure of the lowest detected surface within a footprint, the appropriate range is the distance from the start of the transmit-pulse to the end of the waveform signal, with a correction for the full width of the transmit pulse impulse response. This elevation can be approximated by:

[geolocated bounce point elevation] + 2[transmit pulse centroid]– [distance to end of waveform signal]* (8)

These calculations assume the laser vector is at nadir. For off-nadir pulses, the distances along the laser vector to the centroids and end of signal should be modified by multiplying by the cosine of the off-nadir pointing angle, although this modification is very small for the near-nadir SLA observations.

The waveform processing and resulting products thus provide a means to correct the SLA first return elevation to a mean elevation for illuminated surfaces, a mean elevation of the last return, and the elevation of the lowest return. The appropriate use of these elevations will depend on the assumed character of the surface within the laser footprint and the intent of the user.

5. CONCLUSIONS

SLA has served as a pathfinder experiment motivating the development of geolocation methodologies and waveform processing algorithms for spaceborne laser altimetry. In particular, the SLA flights motivated the use of the ocean reference surface for determination of laser altimeter timing, range, and pointing biases. The first collection of globally distributed laser altimeter waveforms has also contributed significantly to the development of signal processing techniques for derivation of surface elevations. The capabilities developed for SLA form the basis of expanded techniques that will be used operationally as part of the upcoming VCL and ICESat laser altimeter missions. The comprehensive data set produced for the SLA-02 mission also provides the science community interested in characterization of Earth topography and land cover properties an opportunity to gain experience with laser altimeter waveform data in preparation for the upcoming missions. Data and in-depth documentation is accessible though the SLA-02 Data Products Webpage, at http://denali.gsfc.nasa.gov:8001/.

6. ACKNOWLEDGEMENTS

The SLA team consisted of a large number of individuals who made this pathfinder experiment possible, lead by Jim Garvin and Jack Bufton. Bryan Blair and David Rabine provided invaluable expertise on the flight acquisition data system and structures. Flight of the SLA instrument was made possible by the infrastructure and personnel of the Shuttle Small Payloads Hitchhiker Program. Funding and hardware for SLA was provided by the NASA Earth Science Enterprise, the Goddard Director's Discretionary Fund, and the ICESat and Mars Observer Laser Altimeter projects.

7. REFERENCES

Bevington, P.R. and D.K. Robinson, 1992. Data Reduction and Error Analysis for the Physical Sciences. Mc Graw Hill, Inc., 2nd Edition, pp. 141-167.

Bufton, J.L., J.B. Blair, J. Cavanaugh, J.B. Garvin, D. J. Harding, D. Hopf, K. Kirks, S. Rabine, and N. Walsh, 1995. Shuttle Laser Altimeter (SLA): a pathfinder for space-based laser altimetry and lidar, Proc. *Shuttle Small Payloads Symposium*, NASA CR-3310, pp. 83-91.

Bufton, J.L., D.H. Harding, and J.B. Garvin, 1999. Shuttle Laser Altimeter: Mission Results and Pathfinder Accomplishments, Proc. *Shuttle Small Payloads Symposium*, in press.

Garvin, J., J. Blair, J. Bufton, and D. Harding, 1996. The Shuttle Laser Altimeter (SLA-01) Experiment: Topographic Remote Sensing of Planet Earth. EOS Trans., AGU, Vol. 77 (7), p. 239.

Garvin, J., J. Bufton, J. Blair, D. Harding, S. Luthcke, J. Frawley, and D. Rowlands, 1998. Observation of the Earth's Topography from Shuttle Laser Altimeter (SLA): Laser-pulse Echo-recovery Measurements of Terrestrial Surfaces, Phys. Chem. Earth, 23(9-10), pp. 1053-1068.

Lemoine, F.G., S.C. Kenyon, J.K. Factor, R.G. Trimmer, N.K. Pavlis, D.S. Chin, C.M. Cox, S.M. Klosko, S.B. Luthcke, M.H. Torrence, Y.M. Wang, R.G. Williamson, E.C. Pavlis, R.H. Rapp, and T.R. Olson, 1998. The Development of the Joint NASA GSFC and the National Imagery and Mapping Agency (NIMA) Geopotential Model EGM96, NASA/TP-1998-206861.

Luthcke, S.B., J.A. Marshall, S.C. Rowton, K.E. Rachlin, C.M. Cox, and R.G. Williamson, 1997. Enhanced Radiative Force Modeling of the Tracking and Data Relay Satellites, The Journal of the Astronautical Sciences, 45(3): 349-370.

Luthcke, S.B., D.D. Rowlands, J.J. McCarthy, E.Stoneking, and D.E. Pavlis, 1999. Spaceborn laser altimeter pointing bias calibration from range residual analysis, submitted to The Journal of Spacecraft and Rockets.

Schrama, E.J.O. and R.D. Ray, 1994. A Preliminary Tidal Analysis of TOPEX/POSEIDON Altimetry, Journal of Geophysical Research, 99(C-12), pp.24, 799-24,808.

Rowlands, D.D., J.A. Marshall, J.J. McCarthy, S.C.Rowton, D. Moore, D.E.Pavlis, S.B. Luthcke, and L.S. Tsaoussi, 1993. GEODYN-II System Description, Hughes STX Contractor Report, Greenbelt, MD-USA.

Rowlands, D.D., S.B. Luthcke, J.A. Marshall, C.M. Cox, R.G. Williamson, and S.C.Rowton, 1997. Space Shuttle Precision Orbit Determination in Support of SLA-1 Using TDRSS and GPS Tracking Data, The Journal of the Astronautical Sciences, 45(1), pp. 113-129.

Yi, Yuchan, 1995. Determination of Gridded Mean Sea Surface from TOPEX, ERS-1 and GEOSAT Altimeter Data, Ohio State University, Department of Geodetic Science and Surveying, Report No. 434, OH-USA.